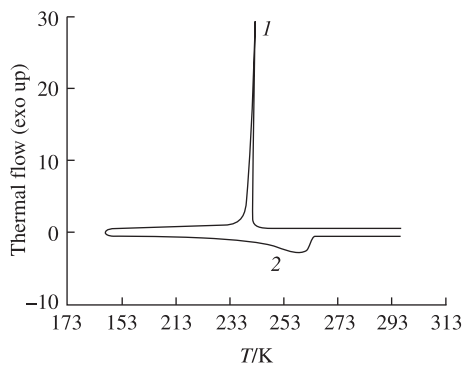


**Figure 1** A model of the phase diagram of the H<sub>2</sub>O–EG–DMSO system with unfolded diagrams of the binary systems H<sub>2</sub>O–EG, H<sub>2</sub>O–DMSO and EG–DMSO.

To construct a fragment of the phase diagram for the system (Figure 1), we used compositions with a constant H<sub>2</sub>O : EG ratio, to which DMSO was added. The H<sub>2</sub>O : EG ratio varied with a step of ~10 mol%, and the DMSO concentration increased by ~10 mol% in each of the sections. In total, ~100 samples were prepared, and thermograms were recorded for all of them. The thermograms manifested exothermic peaks upon cooling the samples at a rate of 3 K min<sup>-1</sup> and endothermic peaks upon subsequent heating at a rate of 3 K min<sup>-1</sup>. The thermogram of a sample containing 34.56 mol% H<sub>2</sub>O, 4.16 mol% EG and 61.28 mol% DMSO is shown in Figure 2. Figure 3 displays a cross-section of the phase diagram of the ternary system built upon heating the crystallized samples. Phase transition temperatures and enthalpy changes in the H<sub>2</sub>O–EG–DMSO system are presented in Table S2, see Online Supplementary Materials.



**Figure 2** Thermogram of a sample containing 34.56 mol% H<sub>2</sub>O, 4.16 mol% EG and 61.28 mol% DMSO, showing (1) exothermic and (2) endothermic peaks corresponding to crystallization and melting of the sample, respectively.

Because of the strong supercooling of the samples, we were unable to obtain the complete phase diagram of the H<sub>2</sub>O–EG–DMSO system from the experimental data (188 K is the temperature limit for the TA Instruments Q100 differential scanning calorimeter); therefore, Figure 1 shows a model of the phase state diagram of the H<sub>2</sub>O–EG–DMSO system based on the diagrams of binary systems. Thin straight lines show the triangulation of the H<sub>2</sub>O–EG–DMSO concentration triangle, which allows describing six subsolidus phase equilibria in the ternary system: ice (H<sub>2</sub>O)–H<sub>2</sub>O–EG–DMSO·3H<sub>2</sub>O (I), EG–H<sub>2</sub>O–EG–DMSO·2EG (II), H<sub>2</sub>O–EG–DMSO·3H<sub>2</sub>O–DMSO·2EG (III), DMSO·3H<sub>2</sub>O–DMSO·2.5H<sub>2</sub>O–DMSO·2EG (IV), DMSO·2.5H<sub>2</sub>O–DMSO·0.5H<sub>2</sub>O–DMSO·2EG (V) and DMSO·0.5H<sub>2</sub>O–DMSO·2EG–DMSO (VI).

The existence of DMSO·2.5H<sub>2</sub>O and DMSO·0.5H<sub>2</sub>O remains an open issue, and the last three equilibria between crystalline

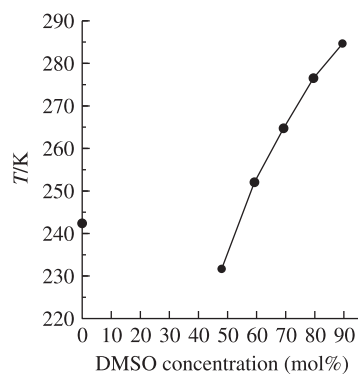


**Figure 3** Section of the phase diagram (30.39 mol% H<sub>2</sub>O + 69.61 mol% EG)–DMSO.

phases can be reduced to one stable equilibrium DMSO·3H<sub>2</sub>O–DMSO·2EG–DMSO. The liquidus surface of the H<sub>2</sub>O–EG–DMSO system is represented by isothermal sections from 210 to 285 K, and simulation based on diagrams of binary systems was carried out for the region of supercooled solutions (see Figure 1, thin curved lines). Peritectic melting of DMSO·2.5H<sub>2</sub>O and DMSO·0.5H<sub>2</sub>O is not considered, and four ternary eutectics E<sub>1</sub>–E<sub>4</sub> with melting below 200 K are presented for the system. Accordingly, the liquidus surface is formed by six surfaces of primary crystallization of H<sub>2</sub>O, EG, DMSO, DMSO·3H<sub>2</sub>O, H<sub>2</sub>O–EG and DMSO·2EG. If peritectics with DMSO·2.5H<sub>2</sub>O and DMSO·0.5H<sub>2</sub>O are realized, then DMSO·2.5H<sub>2</sub>O, DMSO·0.5H<sub>2</sub>O and DMSO·2EG would melt in the E<sub>3</sub> eutectic (DMSO·3H<sub>2</sub>O–DMSO·2EG–DMSO), and two peritectoid equilibrium points, melt–DMSO·3H<sub>2</sub>O–DMSO·2.5H<sub>2</sub>O–DMSO·2EG and melt–DMSO·0.5H<sub>2</sub>O–DMSO–DMSO·2EG, would be located near E<sub>3</sub> (see Figure 1, dashed lines near E<sub>3</sub>). Moreover, with a high probability, the following will be realized in the system: metastable states, in which the lowest-temperature metastable eutectic will correspond to ice–EG–DMSO melting; the glass formation region, which can range from H<sub>2</sub>O–DMSO<sup>5</sup> to EG–DMSO;<sup>11</sup> and the delamination region, which begins in the EG–DMSO system.<sup>11</sup>

Thus, thermograms demonstrate no thermal effects observed in the H<sub>2</sub>O–EG–DMSO system (see Figure 1) in the composition range from 10 to ~50 mol% DMSO upon cooling to 188 K, which indicates the existence of a broad region of supercooled solutions. Keeping for 60 min did not lead to the formation of a crystalline phase. The effect of lowering the low-temperature limit of the existence of solutions can be explained by the formation of mixed networks of hydrogen bonds of water and ethylene glycol with a noticeable strengthening of intermolecular interactions, which create an energy barrier that prevents the crystallization of solution components.

The studied three-component system H<sub>2</sub>O–EG–DMSO can be attributed to systems that exist as solutions in a wide range at low temperatures and can be used in cryobiology.

This work was supported by the Ministry of Science and Higher Education of the Russian Federation (State Assignment to the N. S. Kurnakov Institute of General and Inorganic Chemistry

of the Russian Academy of Sciences) and the Russian Foundation for Basic Research (project no. 19-03-00215). The authors are incredibly grateful to Dr. G. D. Nipan, Doctor of Chemical Sciences, for discussing the work and valuable comments.

#### Online Supplementary Materials

Supplementary data associated with this article can be found in the online version at doi: 10.1016/j.mencom.2021.11.041.

#### References

- 1 G. D. Elliott, S. Wang and B. J. Fuller, *Cryobiology*, 2017, **76**, 74.
- 2 R. Raju, S. J. Bryant, B. L. Wilkinson and G. Bryant, *Biochim. Biophys. Acta, Gen. Subj.*, 2021, **1865**, 129749.
- 3 Z. Hubálek, *Cryobiology*, 2003, **46**, 205.
- 4 Y. P. Klapshin, I. A. Solonina, M. N. Rodnikova, M. R. Kiselev, A. V. Khoroshilov and S. V. Makaev, *Mendeleev Commun.*, 2020, **30**, 534.
- 5 D. H. Rasmussen and A. P. Mackenzie, *Nature*, 1968, **220**, 1315.
- 6 *ASTM Method D-1177-93a, Standard Test Method for Freezing Point of Aqueous Engine Coolant*, American Society for Testing and Materials, Philadelphia, PA, 1993.
- 7 D. R. Cordray, L. R. Kaplan, P. M. Woyciesjes and T. F. Kozak, *Fluid Phase Equilib.*, 1996, **117**, 146.
- 8 M. Matsugami, T. Takamuku, T. Otomo and T. Yamaguchi, *J. Phys. Chem. B*, 2006, **110**, 12372.
- 9 A. V. Zinchenko and V. A. Moiseev, *Kriobiologiya (Cryobiology)*, 1986, no. 4, 25 (in Russian).
- 10 J. B. Ott, J. R. Goates and J. D. Lamb, *J. Chem. Thermodyn.*, 1972, **4**, 123.
- 11 I. A. Solonina, M. N. Rodnikova, M. R. Kiselev, A. V. Khoroshilov and E. V. Shirokova, *Russ. J. Phys. Chem. A*, 2018, **92**, 918. (*Zh. Fiz. Khim.*, 2018, **92**, 751).
- 12 M. N. Rodnikova, *Russ. J. Phys. Chem. A*, 1993, **67**, 248 (*Zh. Fiz. Khim.*, 1993, **67**, 275).
- 13 G. M. Agayan, N. K. Balabaev and M. N. Rodnikova, *Russ. J. Phys. Chem. A*, 2021, **95**, 1283 (*Zh. Fiz. Khim.*, 2021, **95**, 963).
- 14 E. G. Kononova, M. N. Rodnikova, I. A. Solonina and E. V. Shirokova, *Russ. J. Phys. Chem. A*, 2020, **94**, 2233 (*Zh. Fiz. Khim.*, 2020, **94**, 1624).
- 15 E. B. Moore and V. Molinero, *Nature*, 2011, **479**, 506.
- 16 M. N. Rodnikova, F. M. Samigullin, I. A. Solonina and D. A. Sirotkin, *J. Struct. Chem.*, 2014, **55**, 256 (*Zh. Strukt. Khim.*, 2014, **55**, 276).

Received: 29th April 2021; Com. 21/6550